

AN EFFECTIVE LOGARITHMIC FINITE ELEMENT FOR FLOW NEAR A WELL

Tan Liu, Daniel Swenson

Kansas State University
Mechanical and Nuclear Engineering Department
Manhattan, KS, 66506 USA
e-mail: swenson@ksu.edu

ABSTRACT

We present a new finite element that incorporates a logarithmic shape function in the radial direction. The element was derived to be used when calculating flows near wells, where the single phase analytic solution has a logarithmic pressure distribution. Using this element, the well can be represented as a point in the mesh and the numerical calculation of pressures and flows near wells is ensured to be accurate.

For a single well test case, calculated pressures have an error of less than one tenth of one percent compared to the analytic solution. This demonstrates that it is possible to use large elements in the vicinity of the well, but still obtain an accurate result.

BACKGROUND

Analytic Solution

For single-phase, steady-state radial flow the solution for pressure is given by:

$$p(r) = p_o + \frac{q_w \mathbf{m}}{2\pi k z} \ln(r_o/r) \quad \text{Eqn. 1}$$

where q_w is the well flow rate (negative for production), \mathbf{m} is the viscosity, k is the permeability, z is the thickness, and r_o is an outer radius at which the pressure p_o is known. If instead of the flow rate, the pressures are known at the well and an outer radius, then the solution is given by:

$$p(r) = p_o - \frac{(p_o - p_w)}{\ln(r_o/r_w)} \ln(r_o/r) \quad \text{Eqn. 2}$$

where p_w is the pressure at the well. For a fracture where flow is assumed to be between parallel plates, $k = a^2/12$ and $z = a$, where a is the fracture

aperture. In all cases, the pressure has a logarithmic distribution in the radial direction.

Numerical Approaches to Approximation

In finite element or finite difference solutions, two approaches can be used to accurately solve such problems numerically. One approach is to actually model the well radius in the mesh, using a fine grid around the well. Such an approach leads to a very fine mesh around the well, since several elements (grid cells) will be required around the circumference of the well. To keep the aspect ratio of the elements (grid cells) reasonable this means that the radial dimension of the cells near the well be a some fraction of the well circumference. Radial grading of the mesh can be used to transition to larger elements (grid cells) but many elements will still be required around a well. In a 2D solution such an approach is feasible, however, in a 3D model the requirement of such a fine mesh around the well becomes excessive.

The alternate approach is to use a coarse grid, but account for the logarithmic distribution near the well in some other manner.

In finite difference modeling of reservoirs a standard method of incorporating the logarithmic distribution is to use the approximation described by Peaceman (1978) to calculate a radius at which the cell pressure is equal to the pressure given by Eqn. 1. For a regular five-point grid, this radius is given by:

$$r = 0.208h \quad \text{Eqn. 3}$$

where h is the grid cell spacing. This factor is appropriate for wells centered in a cell. Other factors can be used for different well locations in a cell, nonsquare grids, or situations where the well is near either a boundary or another well (Maizeret, 1996).

In the finite element method, approaches have been developed to include the desired approximation in the element. Since the analytic solution is then included in the solution space, the exact solution will be recovered in the finite element solution. This

approach has been used most often for fracture problems, where the stress near the crack tip has a $1/\sqrt{r}$ singularity.

Tharp (1982) discusses an enriched four-node element which models the logarithmic head distribution. The element used the standard bilinear quadrilateral shape functions. He added a fifth node in the center of the element that had a corresponding logarithmic shape function:

$$N_5 = (1-t^2)(1-s^2) \frac{\ln(r_e/r)}{\ln(r_e/r_w)} \quad \text{Eqn. 3}$$

where $2r_e$ is equal to the side length of the square element. The original bilinear shape functions were modified by:

$$N'_i = N_i(s,t) - N_i(0,0)N_5(s,t) \quad \text{Eqn. 4}$$

In the paper, this modification was based on the argument that the logarithmic distribution vanishes as the local head approaches the assigned well head. Alternately, the modification of the original shape functions can be seen as necessary to satisfy the fundamental interpolation property that the original shapes functions vanish at node 5:

$$N_a(0,0) = 0, \quad a = 1, 2, \dots, 4 \quad \text{Eqn. 5}$$

or more generally (Hughes, 1980),

$$N_a(s_b, t_b) = \mathbf{d}_{ab}, \quad a, b = 1, 2, \dots, n \quad \text{Eqn. 6}$$

where n is the number of nodes in the element. Using this element, Tharp obtained accuracies between 1 and 5% when comparing to known analytical solutions. This accuracy is very reasonable given the approximations in element radius and integration.

Xue (1985) presents a much more complex approach in which a circular region surrounding the well is subdivided into a spiral of triangles with curved and straight sides. Using a transformation, these elements that define a circle (cylinder in 3D) around the well are mapped to a rectangle (hexahedron in 3D). The mapping leads to a logarithmic approximation in the original system, satisfying the solution near the well.

Using this approach, Xue obtained results with accuracies of 5 to 10% when compared to Neuman's solution for drawdown at a pumping well.

DERIVATION OF NEW ELEMENT

Approach

The goal is to develop an element that allows the use of a coarse grid around a well, while still accurately calculating the local logarithmic pressure distribution. An example mesh is shown in Figure 1, where the well is a point in the mesh and a rosette of logarithmic elements surrounds the well. We use this mesh to calculate flow in planar fractures intersected by a well, but the element derivation is also applicable to flow in porous media where the well would be a line source.

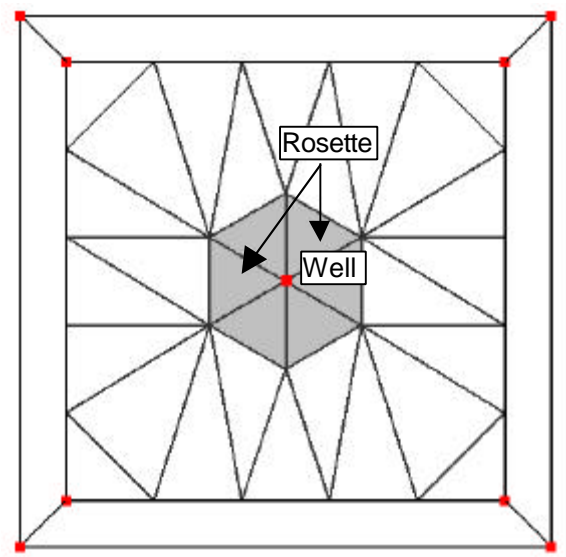


Figure 1: Finite element mesh showing well as a point surrounded by a rosette of logarithmic elements

The fluid flow elements outside the rosette are standard six-noded elements with quadratic shape functions (T6). The logarithmic elements must be compatible with these standard elements on the outer edges of the rosette.

Although in the mesh the logarithmic element appears as a T6 triangle, it is actually implemented as an eight-noded quadrilateral (Q8) element created using the T6 triangle geometry. The edge adjacent to the well uses the well radius to define the Q8 nodes. Figure 2 shows the relationships between the T6 nodes (unprimed) and the Q8 element nodes (primed).

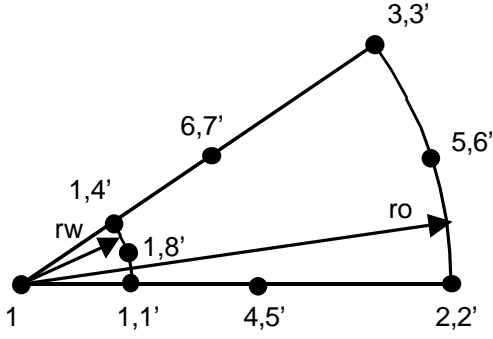


Figure 2: Node numbering for T6 (unprimed) and Q8 (primed) logarithmic elements

1D Logarithmic Element

The first step to derive a logarithmic 1D element that will then be used to develop the 2D element. This element is constructed using the algorithm given by Hughes and Akin, 1980.

We choose as our preliminary shape functions:

$$N_2^p = (1 - s)$$

$$N_3^p = s$$

Eqn. 7

which satisfy the interpolation property (Eqn. 6) at $s_2 = 0$ and $s_3 = 1$. We then add a logarithmic shape function:

$$N_1 = \ln(r_o/r)$$

Eqn. 8

where:

$$r = -\frac{s}{2}(1-s)r_w + (1-s^2)r_2 + \frac{s}{2}(1+s)r_0$$

Eqn. 9

with

$$r_2 = \frac{r_o}{2}$$

Eqn. 10

We modify the shape functions as follows:

$$N_1^{\ln} = \frac{N_1(s) - N_1(0)N_2^p(s) - N_1(1)N_3^p(s)}{N_1(-1) - N_1(0)N_2^p(-1) - N_1(1)N_3^p(-1)}$$

$$N_2^{\ln}(s) = N_2^p(s) - N_2^p(-1)N_1(s)$$

$$N_3^{\ln}(s) = N_3^p(s) - N_3^p(-1)N_1(s)$$

Eqn. 11

or:

$$N_1^{\ln} = \frac{\ln(r_o/r) - \ln(r_o/r_2)(1-s)}{\ln(r_o/r_w) - 2\ln(r_o/r_2)}$$

$$N_2^{\ln} = 1 - s - 2 \frac{\ln(r_o/r) - \ln(r_o/r_2)(1-s)}{\ln(r_o/r_w) - 2\ln(r_o/r_2)}$$

$$N_3^{\ln} = s + \frac{\ln(r_o/r) - \ln(r_o/r_2)(1-s)}{\ln(r_o/r_w) - 2\ln(r_o/r_2)}$$

Eqn. 12

Figure 3 shows a graph of the three 1D logarithmic shape functions. Figure 4 shows how these shape functions can exactly represent constant, linear, and logarithmic solutions. A standard 3-noded quadratic element can exactly represent constant, linear, and quadratic solutions. Our modification to the standard element has introduced the logarithmic representation. Since the logarithmic representation is now in the solution space, the final solution will include this term near a well.

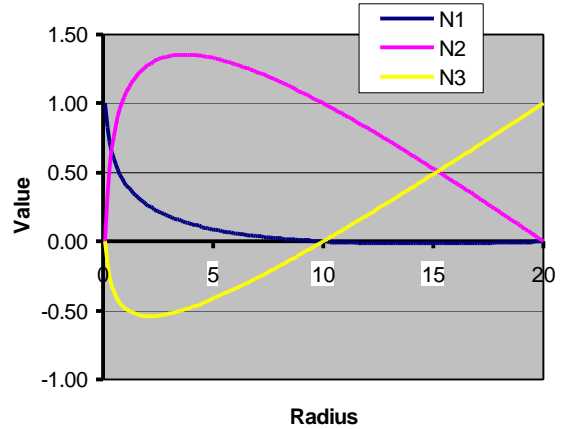


Figure 3: 1D logarithmic shape functions

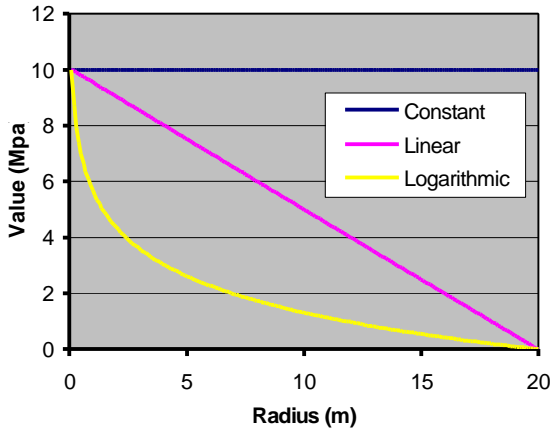


Figure 4: Constant, linear, and logarithmic functions using 1D logarithmic shape functions

2D Logarithmic Element

The 2D logarithmic element is derived by first creating a 6-noded quadrilateral element formed as the products of the 1D logarithmic shape functions in the radial direction and the standard 1D linear shape functions in the circumferential direction, Figure 5.

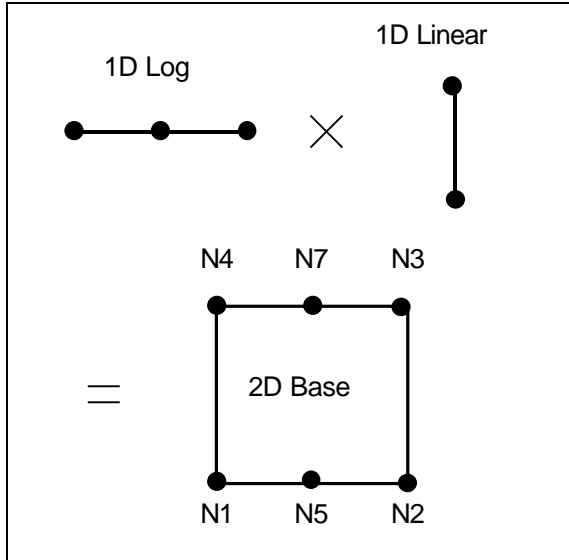


Figure 5: Forming base 2D element as product of 1D logarithmic and linear shape functions

This element could be used in a rosette around the well and would be compatible with standard linear elements surrounding the rosette. In our application, we use quadratic elements to surround the rosette, so we add two additional nodes and corresponding shape functions so that the logarithmic element has quadratic shape functions on the outer edge. To do this, we again follow the approach described by Hughes, 1987, for elements with variable number of nodes.

We first add the N6 shape function on the outer edge of the element:

$$N6' = \frac{1}{2}(1+s)(1-t^2) \quad \text{Eqn. 13}$$

where s is the natural coordinate in the radial direction and t is in the circumferential direction. This shape function is the standard serendipity element shape function and is zero at all other nodes. We then correct the shape functions shown in Figure 5 to satisfy the interpolation condition. Finally, we construct the N8 shape function as:

$$N8 = \frac{\ln(r_0/r)}{\ln(r_0/r_w)}(1-t^2) \quad \text{Eqn. 14}$$

This is also zero at all nodes so we correct the seven existing shape functions to satisfy the interpolation condition. The final result gives eight shape functions defined as follows:

$$N_1 = \frac{(1-t)}{2} \frac{\ln(r_0/r) - \ln(r_0/r_2)(1-s)}{\ln(r_0/r_w) - 2\ln(r_0/r_2)} - \frac{(1-t^2)}{2} \frac{\ln(r_0/r)}{\ln(r_0/r_w)}$$

$$N_2 = \frac{(1-t)}{2} \frac{\ln(r_0/r) - \ln(r_0/r_2)(1-s)}{\ln(r_0/r_w) - 2\ln(r_0/r_2)} - \frac{(1-t^2)(1+s)}{4}$$

$$N_3 = \frac{(1+t)}{2} \left(s + \frac{\ln(r_0/r) - \ln(r_0/r_2)(1-s)}{\ln(r_0/r_w) - 2\ln(r_0/r_2)} \right) - \frac{(1-t^2)(1+s)}{4}$$

$$N_4 = \frac{(1+t)}{2} \frac{\ln(r_0/r) - \ln(r_0/r_2)(1-s)}{\ln(r_0/r_w) - 2\ln(r_0/r_2)} - \frac{(1-t^2)}{2} \frac{\ln(r_0/r)}{\ln(r_0/r_w)}$$

$$N_5 = \frac{(1-t)}{2} \left(1 - s - 2 \frac{\ln(r_0/r) - \ln(r_0/r_2)(1-s)}{\ln(r_0/r_w) - 2\ln(r_0/r_2)} \right)$$

$$N_6 = \frac{(1+s)}{2} (1-t^2)$$

$$N_7 = \frac{(1+t)}{2} \left(1 - s - 2 \frac{\ln(r_0/r) - \ln(r_0/r_2)(1-s)}{\ln(r_0/r_w) - 2\ln(r_0/r_2)} \right)$$

$$N_8 = (1-t^2) \frac{\ln(r_0/r)}{\ln(r_0/r_w)} \quad \text{Eqn. 15}$$

Using the definition

$$r' = \frac{dr}{ds} = (s - 0.5)r_w - 2sr_2 + (0.5 + s)r_0$$

Eqn. 16

the derivatives of the shape functions are given by:

$$\frac{\partial N_1}{\partial s} = \frac{1}{2} \left(\frac{-r'/r + \ln(r_0/r_2)}{\ln(r_0/r_w) - 2\ln(r_0/r_2)} (1-t) + \frac{r'/r}{\ln(r_0/r_w)} (1-t^2) \right)$$

$$\frac{\partial N_2}{\partial s} = \frac{1}{2} \left(1 + \frac{-r'/r + \ln(r_0/r_2)}{\ln(r_0/r_w) - 2\ln(r_0/r_2)} \right) (1-t) - \frac{(1-t^2)}{4}$$

$$\frac{\partial N_3}{\partial s} = \frac{1}{2} \left(1 + \frac{-r'/r + \ln(r_0/r_2)}{\ln(r_0/r_w) - 2\ln(r_0/r_2)} \right) (1+t) - \frac{(1-t^2)}{4}$$

$$\frac{\partial N_4}{\partial s} = \frac{1}{2} \left(\frac{-r'/r + \ln(r_0/r_2)}{\ln(r_0/r_w) - 2\ln(r_0/r_2)} (1+t) + \frac{r'/r}{\ln(r_0/r_w)} (1-t^2) \right)$$

$$\frac{\partial N_5}{\partial s} = -1 - \frac{-r'/r + \ln(r_0/r_2)}{\ln(r_0/r_w) - 2\ln(r_0/r_2)} (1-t)$$

$$\frac{\partial N_6}{\partial s} = \frac{1}{2} (1-t^2)$$

$$\frac{\partial N_7}{\partial s} = -1 - \frac{-r'/r + \ln(r_0/r_2)}{\ln(r_0/r_w) - 2\ln(r_0/r_2)} (1+t)$$

$$\frac{\partial N_8}{\partial s} = -\frac{r'/r}{\ln(r_0/r_w)} (1-t^2)$$

Eqn. 17

and:

$$\frac{\partial N_1}{\partial t} = -\frac{1}{2} \left(\frac{\ln(r_0/r) - \ln(r_0/r_2)(1-s)}{\ln(r_0/r_w) - 2\ln(r_0/r_2)} \right) + \frac{\ln(r_0/r)}{\ln(r_0/r_w)} t$$

$$\frac{\partial N_2}{\partial t} = \frac{1}{2} \left(-\frac{\ln(r_0/r) - \ln(r_0/r_2)(1-s)}{\ln(r_0/r_w) - 2\ln(r_0/r_2)} + t + st - s \right)$$

$$\frac{\partial N_3}{\partial t} = \frac{1}{2} \left(\frac{\ln(r_0/r) - \ln(r_0/r_2)(1-s)}{\ln(r_0/r_w) - 2\ln(r_0/r_2)} + t + st + s \right)$$

$$\frac{\partial N_4}{\partial t} = \frac{1}{2} \left(\frac{\ln(r_0/r) - \ln(r_0/r_2)(1-s)}{\ln(r_0/r_w) - 2\ln(r_0/r_2)} \right) + \frac{\ln(r_0/r)}{\ln(r_0/r_w)} t$$

$$\frac{\partial N_5}{\partial t} = \frac{s-1}{2} + \frac{\ln(r_0/r) - \ln(r_0/r_2)(1-s)}{\ln(r_0/r_w) - 2\ln(r_0/r_2)}$$

$$\frac{\partial N_6}{\partial t} = -t - st$$

$$\frac{\partial N_7}{\partial t} = \frac{1-s}{2} - \frac{\ln(r_0/r) - \ln(r_0/r_2)(1-s)}{\ln(r_0/r_w) - 2\ln(r_0/r_2)}$$

$$\frac{\partial N_8}{\partial t} = -2t \frac{\ln(r_0/r)}{\ln(r_0/r_w)}$$

Eqn. 18

Plots of selected shape functions are shown in Figure 6, Figure 7, and Figure 8.

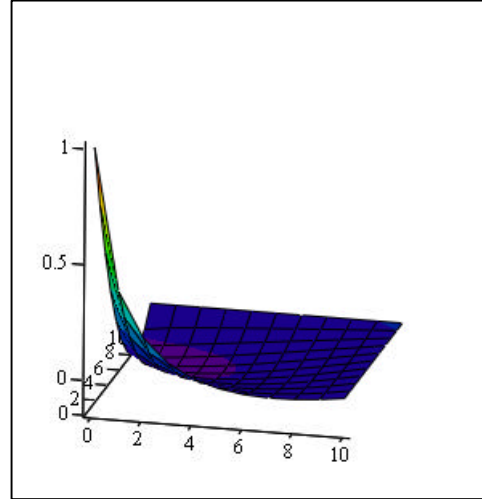


Figure 6: Plot of N_1

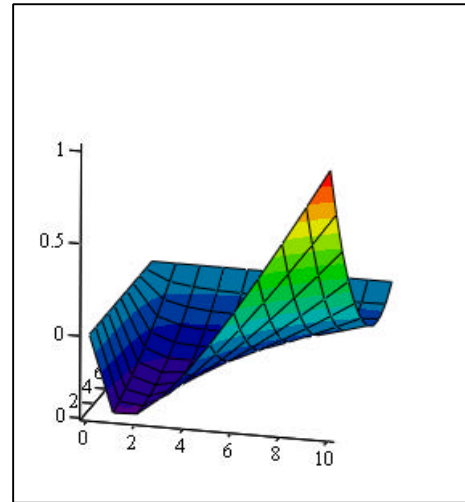


Figure 7: Plot of N_2

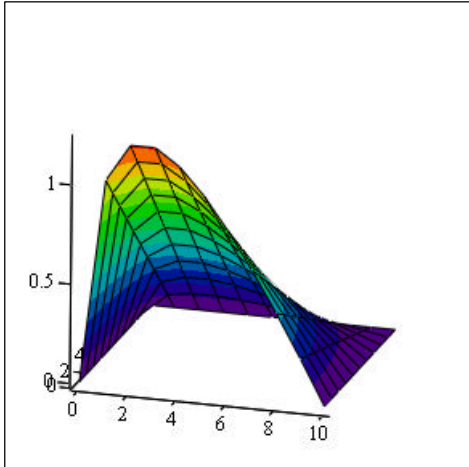


Figure 8: Plot of N_5

Integration of Stiffness Matrix

Because of the logarithmic terms, care must be taken to ensure accuracy. Integration is performed using an adaptive scheme in the radial direction and standard three gauss point integration in the circumferential direction.

Use of Element

As shown in Figure 2, to the external mesh, the logarithmic well element uses the geometry of a six-noded triangular element. To calculate the stiffness matrix, an eight-noded quadrilateral element is formed, using the well radius to define one edge. The stiffness matrix of this Q8 element is calculated. During assembly of the global stiffness matrix, the Q8 element degrees of freedom on the well radius are given the same equation number as the T6 element.

Extension to 3D

Extension to 3D prismatic elements is straight forward. These elements can use either linear or quadratic shape functions in the Z direction.

VERIFICATION

A verification problem using a well radius of 0.1 m and an outer radius of 100m was used to demonstrate the accuracy of the logarithmic element, Figure 9. The fracture aperture is 0.5 mm and the dynamic viscosity 0.000125 kg/m-sec. The well pressure is 1.0 MPa and the outer pressure 0.0 MPa. The analytical solution is given by Eqn. 2.

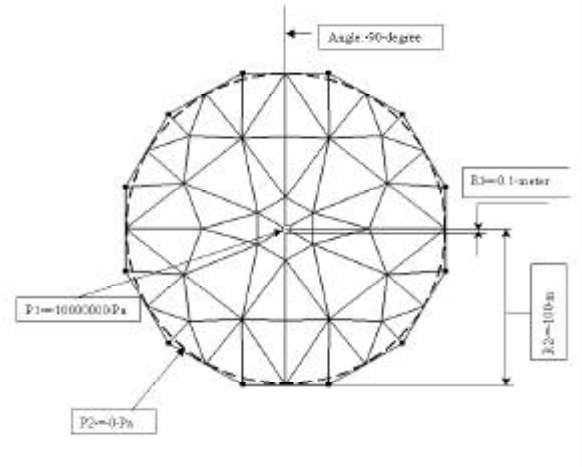


Figure 9: Mesh used for verification problem

Figure 10 shows the pressure contours around the well and Figure 11 shows a comparison of the solution using the logarithmic and standard finite elements. As can be seen, the logarithmic element gives solutions within 0.1 % accuracy. Similar results were obtained for verification when the flow rate was specified, rather than pressure boundary conditions. In that case, the logarithmic solution gave results within 0.1 % accuracy, while the standard finite element gave a pressure at the well of 0.67 MPa, an error of more than 30 %.

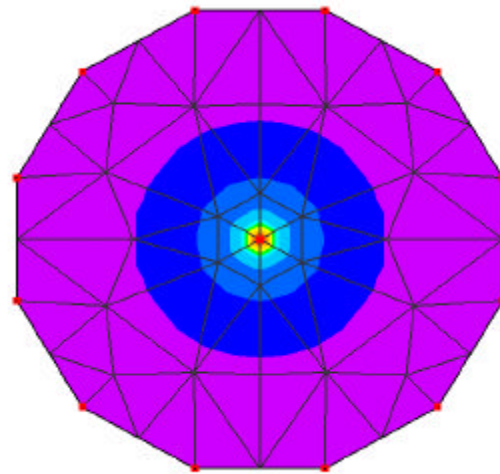


Figure 10: Pressure contours for verification problem

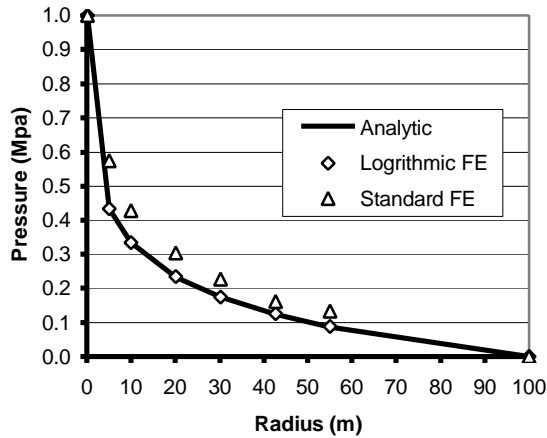


Figure 11: Comparison of logarithmic element and standard element solutions

CONCLUSIONS

The logarithmic element provides a means to accurately calculate the pressures and flows near a well using large elements near the well. Calculated pressures are accurate on the order of 0.1 %. The element has been implemented in the Geocrack3D code.

REFERENCES

- Hughes, T. J. R. and Akin, J. E. (1980), "Techniques for Developing Special Finite Element Shape Functions with Particular Reference to Singularities," *Int. J. for Numerical Methods in Engineering*, Vol. 15, 733-751
- Hughes, T. J. R., 1987, *The Finite Element Method*, Prentice-Hall, Inc., Englewood Cliffs, New Jersey, 07632.
- Maizeret, P. D., (1966), *Well Indices for Non-Conventional Wells*, M. S. Thesis, Stanford University, June.
- Peaceman, D. W., (1978), "Interpretation of Well-Block Pressures in Numerical Reservoir Simulation," *Soc. Pet. Eng. J, Trans. AIME*, 253, June, pp. 183-194.
- Xue, Y., (1985), "Logarithmic finite element interpolation of flow near wells in phreatic aquifers," *Advances in Water Resources*, v. 8, n. 3, Sept. 1985, pp. 111-117.